Kinetic mechanism and ATP-binding site reactivity of p38γ MAP kinase

Ted Fox*, Matthew J. Fitzgibbon, Mark A. Fleming, Hsun-Mei Hsiao, Christopher L. Brummel, Michael S-S. Su

Vertex Pharmaceuticals Incorporated, 130 Waverly Street, Cambridge, MA 02139-4242, USA

Received 27 September 1999; received in revised form 21 October 1999

Abstract Activated p38γ MAP kinase exhibited significant basal ATPase activity in the absence of a kinase substrate, and addition of a phosphoacceptor substrate increased $k_{cat}/K_m > 20$-fold. AMP-PCP was competitive with ATP binding and non-competitive with phosphoacceptor substrate binding. The nucleotide binding site affinity label 5′-(*p*-fluorosulfonylbenzoyl)adenosine (FSBA) bound stoichiometrically at Lys-56 in the ATP site of both unphosphorylated and activated p38γ. AMP-PCP only protected the activated enzyme from FSBA inactivation, implying that AMP-PCP does not bind unphosphorylated p38γ. Basal ATPase activities were also observed for activated p38α, ERK2 and JNK3 suggesting that the enzymatic mechanism may be similar for all classes of MAP kinases.

Key words: MAP kinase; p38γ; Kinetic mechanism; ATPase; ATP-binding site; Kinase; 5′-(*p*-Fluorosulfonylbenzoyl)adenosine

1. Introduction

The mitogen-activated protein (MAP) kinase family are serine/threonine kinases that mediate intracellular signal transduction pathways [1,2]. This family contains three sequence and structurally similar classes of enzymes: the extracellular signal regulated kinases (ERKs), Jun N-terminal kinases (JNKs) and p38 kinases. These kinases are activated by phosphorylation of both threonyl and tyrosyl sidechains arranged in a Thr-X-Tyr motif, where X represents a Glu, Pro and Gly in ERK, JNK and p38 kinases, respectively [1,3]. ERKs are activated by mitogens and growth factors [4], whereas the JNK and p38 kinases are activated in response to pro-inflammatory cytokines and by cellular stress [5–7]. MAP kinases use ATP to phosphorylate various regulatory proteins including 90 kDa ribosomal s6 kinase (Rsk90) and MAPK-activated protein kinase-2 (MAPKAP2) [8], as well as transcription factors such as activating transcription factor 2 (ATF2) [9,10], Elk1 [9,11], c-Fos [12], c-Myc [13], c-Jun [14], NFAT [15] and DENN [16].

p38γ MAP kinase shows 61% amino acid sequence identity with p38α, but is expressed predominantly in skeletal muscle tissue [17,18]. In contrast, p38α is found in a variety of tissues. The different tissue distribution suggests p38γ may have a different function than p38α MAP kinase, although this is not currently known.

This study was designed to analyze the kinetic mechanism and ATP-binding site reactivity of p38γ MAP kinase using ATP analogs. We present data indicative of a mechanism in which substrates bind to p38γ either in a random manner, or possibly in an ordered manner, with ATP binding first. ATP and phosphoacceptor substrates have no observable effect on the binding of one another and the kinetic mechanism is independent of the phosphoacceptor size (i.e. peptide or protein). The non-hydrolyzable ATP analog, β,γ-methyleneadenosine 5′-triphosphate (AMP-PCP), is a competitive inhibitor of ATP binding and a non-competitive inhibitor of epidermal growth factor receptor (EGFR) peptide and GST-ATF2 binding to p38γ. We observe significant basal ATPase activity for all activated p38, ERK and JNK members studied, which eliminates a mechanism requiring that kinase substrate binding precedes ATP binding for any of the MAP kinases in this study.

2. Materials and methods

2.1. Materials

^{14}C-5′-(*p*-fluorosulfonylbenzoyl)adenosine (FSBA) was purchased from NEN Life Science Products (Boston, MA, USA), horse heart myoglobin, AMP-PCP, ATP and FSBA were obtained from Sigma (Saint Louis, MO, USA). SB202190 and SB203580 were purchased from Upstate Biotechnology, Lake Placid, NY, USA.

2.2. Expression of kinases

We obtained an EST clone (#163561) containing the human cDNA encoding p38γ kinase from Research Genetics (Huntsville, AL, USA). A cDNA fragment encoding an N-terminal $(His)_6$ tagged p38γ kinase was amplified by PCR using a pair of forward and reverse primers: 5′-GGATCCATGGGCCATCACCATCACCATCACGCCAGCTCTCCGCCGCCCGG-3′ and 5′-GGATTCGAATTCCTATCACAGAAGGGCGTCTCCTTG-3′. The amplified cDNA fragment was digested with *Nco*I and *Eco*RI and cloned into the expression vector pET-BS(+). *Escherichia coli* BL21(DE3) was transformed with the plasmid pET-BS(+)/$(His)_6$-p38γ and grown at 30°C to an OD_{550} of 0.8–1.0 and protein expression induced with 1 mM IPTG for 3 h. Bacteria were harvested and stored at −70°C prior to use.

2.3. Protein purification

E. coli cell paste expressing $(His)_6$-*p*38γ was resuspended in 10 volumes/g of Buffer A (50 mM HEPES pH 8.0, 200 mM NaCl, 2 mM β-mercaptoethanol (β-ME), 10% glycerol and 0.2 mM phenylmethylsulfonyl fluoride (PMSF)). Following mechanical disruption of the cells in a Microfluidizer (Microfluidics, Newton, MA, USA), the lysate was centrifuged at 30 000×*g* for 30 min at 4°C. The supernatant was incubated batch-wise overnight at 4°C with 1 ml of Talon metal affinity resin (Clontech, Palo Alto, CA, USA) per 5 mg of expected p38γ. The resin was settled by centrifugation at 500×*g* and washed batch-wise with Buffer A at 4°C. The resin was washed with 10 column volumes of buffer A +7.5 mM imidazole. The p38γ was eluted with Buffer A +100 mM imidazole and dialyzed overnight at 4°C vs.

*Corresponding author. Fax: (1) (617) 577-6400.
E-mail: Fox@vpharm.com

Abbreviations: MAP, mitogen-activated protein; ERK, extracellular signal regulated kinase; JNK, Jun N-terminal kinase; EGFR, epidermal growth factor receptor; MKK, MAP kinase kinase; MAPKAP2, MAPK-activated protein kinase-2; ATF2, activating transcription factor 2; RSK90, 90 kDa ribosomal s6 kinase; PMSF, phenylmethylsulfonyl fluoride; DTT, dithiothreitol; β-ME, β-mercaptoethanol; AMP-PCP, β,γ-methyleneadenosine 5′-triphosphate; FSBA, 5′-(*p*-fluorosulfonylbenzoyl)adenosine

0014-5793/99/$20.00
PII: S0014-5793(99)01488-X

50 mM HEPES, pH 7.5, 50 mM NaCl, 5% glycerol, 2 mM dithiothreitol (DTT). The protein was further purified on a MonoQ (HR 10/10) column (Pharmacia, Uppsala, Sweden), as described below, for either unphosphorylated enzyme or following activation. *E. coli* cell paste expressing GST-ATF2 was lysed and centrifuged as described for p38γ (no β-ME in the buffer) and incubated batch-wise with 1 ml glutathione agarose (Sigma, St Louis, MO, USA)/ 5 mg of expected protein for 3 h at 4°C. The resin was washed with 20 column volumes of buffer A and eluted with the same buffer containing 10 mM reduced glutathione at 4°C. GST-ATF2 was further purified by size-exclusion chromatography using a Sephacryl S100 (Pharmacia, Uppsala, Sweden) column equilibrated in buffer A at 4°C using a flow rate of 0.4 ml/min. GST-ATF2 was concentrated in a Centriprep-50 (Amicon, Beverly, MA, USA) to 10–20 mg/ml and stored at −70°C.

2.4. Activation of p38γ

A constitutively active mutant of MAP kinase kinase (MKK)6 was expressed and purified as described [19]. Typically, 10–15 mg of p38γ was diluted to 0.5 mg/ml in buffer B. MKK6(DD) was added at 20 μg/ml and the activation initiated by addition of ATP in six separate 0.5 mM (final concentration) increments at 5 min intervals. After 30 min the activation mixture was filtered through a 0.2 μm filter and applied to a MonoQ (HR 10/10) column (Pharmacia, Uppsala, Sweden) equilibrated in buffer B. The column was washed to baseline with buffer B and eluted with a 20 column volume gradient to buffer B containing 0.4 M NaCl. The activated p38γ peak was pooled, dialyzed at 4°C versus buffer B, and stored at −70°C.

2.5. Kinase assays

A previously described coupled spectrophotometric assay was used to follow ATPase and kinase activities [20]. Reactions were performed in 50 mM HEPES, pH 7.6, 10 mM $MgCl_2$, and started by addition of 15–1000 μM ATP as described. Addition of 0–2 mM of the peptide KRELVEPLTPSGEAPNQALLR, corresponding to an EGF receptor substrate peptide [21], allowed measurement of kinase activity. Alternatively, 0–400 μM GST-ATF2 was added to measure kinase activity. In K_i determinations, enzyme and inhibitor were pre-incubated for 15 min at 30°C prior to assay by ATP addition. Enzyme kinetics analyses were performed by non-linear regression in the program EZ-Fit (Perrella Scientific, Amherst, NH, USA).

2.6. FSBA labeling of MAP Kinases

Two molar equivalents of ^{14}C-FSBA were added to 2.5 μM unphosphorylated or activated MAP kinase at 25°C in 50 mM HEPES, pH 7.6, 10 mM $MgCl_2$ and 2 mM DTT, in the presence or absence of protein or peptide kinase substrate. ATP-binding site competition experiments were performed as above in the presence of 1.2 mM AMP-PCP. Reactions were quenched at various time points by addition of SDS-PAGE sample buffer, and the modified MAP kinases separated by SDS-PAGE, fixed and visualized by phosphorimaging and autoradiography.

2.7. Protein sequencing

Two molar equivalents of FSBA in DMSO were added to 250 μg of unphosphorylated or activated p38γ. Control samples of p38γ were treated with DMSO. Samples were incubated at 25°C for 2 h. Fifty microgram samples were then loaded on a HP1100 HPLC system utilizing a 2×150 mm C_{18} reversed phase column (Phenomenex, Torrance, CA, USA) and a TFA/acetonitrile gradient system. Intact proteins were eluted from the column with a linear gradient, collected and lyophilized for mass spectral analysis. The remaining 200 μg of each sample was exchanged into 50 mM HEPES, pH 7.5, for in vitro proteolysis. Lys-C protease (8 μg) was added to each sample and incubated at 37°C for 16 h. Peptides were separated as above and the FSBA-modified peptide identified by LC-MS difference maps. The peptide identity was confirmed by traditional N-terminal protein sequencing.

2.8. Mass spectral analysis of purified proteins

Electrospray mass spectra of protein samples were collected using a Micromass Quattro II triple quadrupole mass spectrometer. Lyophilized protein samples were dissolved in a 50:50 (acetonitrile:water) solution with 0.2% formic acid and introduced at a flow rate of 20 μl/min. Data were collected by scanning the first quadrupole with a step size of 8 points per Da and the resolution was adjusted to 0.65 *m/z* over the scanned mass to charge range of 500–2000 *m/z*. The quadrupole was calibrated using horse heart myoglobin before and after p38γ data collection. Data deconvolution was performed using the MassLynx software BioTools (Micromass, Bedford, MA, USA).

3. Results

3.1. Activation of p38γ

p38γ was activated using a constitutively active mutant of MKK6, the immediate upstream MAPK kinase responsible for activating p38. In this mutant, the phosphorylation sites, Ser-207 and Thr-211, are substituted with Asp residues [9,22]. A comparison of the molecular weights of unphosphorylated and activated p38γ by mass spectrometry showed an increase of 239 Da, due to phosphorylation at three sites. Digestion of activated p38γ with Lys-C protease, followed by protein sequencing, identified the sites as Tyr-183 and Thr-185, in the activation lip, and Ser-3 near the N-terminal portion of the enzyme. Control experiments demonstrated that activated

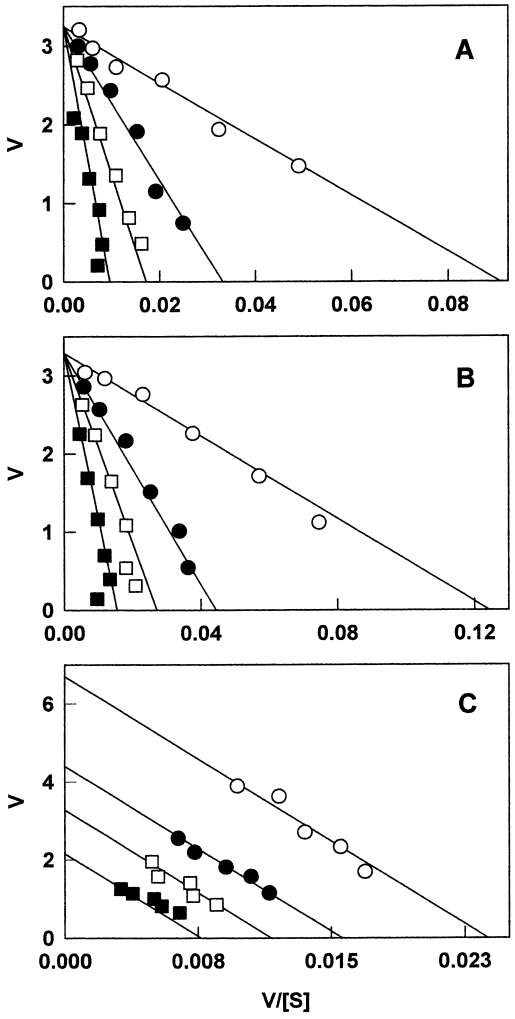

Fig. 1. Eadie-Hofstee plots of *v* (μM/min) versus *v*/[*S*] for AMP-PCP inhibition of activated p38γ MAP kinase. A: ATPase activity at 15–500 μM ATP in the presence of 0 (○), 300 (●), 600 (□) and 1200 (■) μM AMP-PCP. B: Kinase activity versus [ATP] at 200 μM GST-ATF2 in the presence of 0 (○), 300 (●), 600 (□) and 1200 (■) μM AMP-PCP. C: Kinase activity versus GST-ATF2 at 120 μM ATP in the presence of 0 (○), 300 (●), 600 (□) and 1200 (■) μM AMP-PCP. See Section 2 for more details.

Table 1
Kinetic constants and mode of inhibition for activated p38γ-catalyzed basal ATPase and kinase reactions

Activity	Substrate		k_{cat} (s^{-1})	K_M (μM)	k_{cat}/K_M (M^{-1} s^{-1})	Inhibition constants (μM)		Inhibition pattern[a]
	Fixed	Varied				K_{is}	K_{ii}	
ATPase	–	ATP	0.33 ± 0.04	37 ± 3.6	8 900	125 ± 15	–	C
Kinase	EGFR	ATP	12.4 ± 0.75	54 ± 9.0	230 000	121 ± 20	–	C
Kinase	ATP	EGFR	14.4 ± 0.63	313 ± 30	46 000	–	372 ± 28	NC
Kinase	GST-ATF2	ATP	5.4 ± 0.14	27 ± 1.0	200 000[b]	177 ± 13	–	C
Kinase	ATP	GST-ATF2	5.5 ± 0.21	254 ± 24	21,650	–	590 ± 20	NC

[a]C = competitive inhibition and NC = non-competitive inhibition
[b]Does not represent a true k_{cat}/K_M because GST-ATF2 is not present at saturating concentrations

p38γ was responsible for phosphorylation at Ser-3 and that this phosphorylation has no effect on the enzymatic activity of p38γ.

3.2. ATPase activity of activated p38γ

ATP was hydrolyzed by activated p38γ in the absence of a phosphoacceptor with a K_m of 37 μM and a k_{cat} of 0.33 s^{-1} for ATP, which yielded a k_{cat}/K_m of 8900 $M^{-1}s^{-1}$ (Table 1). AMP-PCP, a hydrolysis-resistant ATP analog, was a competitive inhibitor of ATP (K_{is} = 125 μM) as shown by an Eadie-Hofstee plot for AMP-PCP inhibition (Fig. 1A). These findings demonstrate that a phosphoacceptor substrate was not required for ATP or AMP-PCP binding to activated p38γ.

3.3. Kinase activity of activated p38γ

Addition of an EGFR peptide substrate during ATP turnover by p38γ yielded a 26-fold increase in k_{cat}/K_m compared to the basal ATPase activity (Table 1). The K_m's for ATP binding in the kinase and ATPase reactions were similar, indicating that the enhanced kinase specificity constant was primarily due to a 38-fold increase in k_{cat}. Similarly, GST-ATF2 stimulated the activity of p38γ (22-fold) due mainly to an increase in k_{cat} (Table 1). The binding synergy between the two substrates was determined from the ratio of $K_{m\ MgATP}$(ATPase)/$K_{m\ MgATP}$(kinase), and was 0.7 for the EGFR peptide, and 1.4 when GST-ATF2 is the phosphoacceptor. These findings demonstrate a lack of binding synergy between ATP and the phosphoacceptor substrates for p38γ MAP kinase.

The K_m values for EGFR peptide and GST-ATF2 binding to activated p38γ at saturating ATP were similar, 313 and 254 μM, respectively (Table 1). Non-linear regression analyses of AMP-PCP inhibition, as the phosphoacceptor substrate concentration was varied, yielded poor fits for both competitive and uncompetitive inhibition models. Linearizing the fitted data in the form of Eadie-Hofstee plots for varied EGFR peptide or GST-ATF2, at saturating ATP, produced parallel lines for different AMP-PCP concentrations (Fig. 1C). This suggests AMP-PCP acts as a non-competitive inhibitor versus the EGFR peptide and GST-ATF2. A non-competitive mechanism implies that AMP-PCP binds independently of the phosphoacceptor substrate (EGFR peptide or GST-ATF2) and that MgATP is not required to bind first.

3.4. ATPase activity of other activated MAP kinases

The observation of basal ATPase activity for activated p38γ rules out a mechanism requiring phosphoacceptor to bind prior to ATP. This finding is inconsistent with a previously published mechanism for p38α, which suggested that the phosphoacceptor substrate binding had to precede that of ATP [23]. To address whether there are mechanistic differences within the same enzyme family we tested MAP kinases from the p38, ERK and JNK classes for basal ATPase activity. The activated form of every MAP kinase tested exhibited significant basal ATPase activity (Table 2), suggesting that none of these enzymes, at least in vitro, have a kinetic mechanism requiring the phosphoacceptor substrate to bind first. ERK2 and p38α showed the weakest basal ATPase activity, 6and 4-fold lower than p38γ, respectively. Interestingly, JNK3 showed a significantly higher level of basal ATPase activity, 9-fold higher than p38γ and up to 55-fold higher than ERK2 (Table 2).

Mass spectrometry was used to show that the unphosphorylated MAP kinases in this study contain no detectable activated enzyme prior to in vitro activation. Upon in vitro activation and repurification, >95% of the enzyme was activated. These observations are consistent with Western blot analyses (anti-phospho antibodies) and the different chromatographic behavior of the unphosphorylated and activated MAP kinases.

3.5. Affinity labeling by FSBA

p38γ is insensitive to pyridinyl imidazole compounds including SB202190 and SB203580 so we sought other inhibitors to further probe the ATP-binding site.

FSBA is an affinity label for nucleotide binding sites that, unlike the non-hydrolyzable AMP-PCP, binds irreversibly to the sidechain of a critical, conserved Lys residue found in the ATP-binding site of most kinases [24]. FSBA is similar in structure to ATP (Fig. 3). Substrate binding to p38γ MAP kinase was characterized using FSBA. The irreversible modification of the ATP-binding site of p38γ MAP kinase was monitored by ^{14}C-FSBA incorporation into unphosphorylated or activated enzyme, in the presence and absence of AMP-PCP. The FSBA affinity label irreversibly bound to both unphosphorylated and activated p38γ, but reacted more rapidly with unphosphorylated p38γ (compare Fig. 2A and B). The presence of AMP-PCP had no effect on ^{14}C-FSBA incorpo-

Table 2
Kinetic parameters for basal ATPase activities exhibited by activated p38α, p38γ, ERK2 and JNK3

MAP Kinase	k_{cat} (s^{-1})	K_M (μM)	k_{cat}/K_M (M^{-1} s^{-1})
p38α[a]	0.40	170	2 350
p38γ	0.33	37	8 900
ERK2	0.17	118	1 440
JNK3	1.04	13	80 000

[a]p38α data kindly provided by Sam Pazhanisamy (personal communication).

ration for the unphosphorylated enzyme. In contrast, the rate and extent of ^{14}C-FSBA incorporation into activated p38γ was significantly lower with added AMP-PCP (Fig. 2B). The inability of the unphosphorylated p38γ to bind ATP could explain why this enzyme exhibits no basal ATPase or kinase activities. Incubating either form of p38γ with EGFR peptide prior to addition of ^{14}C-FSBA had no effect on the incorporation of the affinity label and did not alter the protective effect of AMP-PCP (not shown). The data in Fig. 2 show that the incorporation of ^{14}C-FSBA was up to 0.6 mol per mol of protein, i.e. sub-stoichiometric, yet the reaction appeared to be leveling off. We suspected this was due to signal quenching in the ^{14}C-FSBA labeling experiments, rather than having a population of protein unable to bind FSBA. We addressed this question by protein sequencing and mass spectral analysis as shown in the next section.

3.6. Protein sequencing and mass spectral analyses of FSBA modified p38γ

The site of FSBA modification on p38γ, as well as the reaction stoichiometry, were identified by incubating either unphosphorylated or activated p38γ with FSBA. The unphosphorylated protein was found to have a molecular weight of 41 573 which is 432 Da higher than unmodified p38γ, indicating the presence of a single FSBA per enzyme (the expected increase is 433 Da). Similarly, for activated p38γ, the molecular weight increased from 41 380 to 41 815 Da upon FSBA modification (i.e. a 435 Da difference). FSBA-modified protein was digested with Lys-C protease and the reversed phase HPLC peptide map compared with that of unmodified p38γ. The overlaid digest maps for p38γ and FSBA-modified p38γ appeared identical except for the shifted retention time of one peptide that exhibited an absorbance peak centered at 245 nm, characteristic of FSBA derivatives [24]. No other peptide peaks showed this absorbance profile. Protein sequencing identified the peptide as VAIKK, although sequence data were not obtained for the fourth cycle in the treated peptide analysis, due to modification of this Lys residue with FSBA. Mass spectrometry confirmed the identity of this modified peptide giving a molecular weight of 990.5 Da, corresponding to the expected mass of covalently bound FSBA (i.e. VAIKK +433 Da). There was no evidence for the presence of unmodified protein in any FSBA-treated samples, which together with the whole protein mass spectral data, strongly suggest that all the p38γ is competent to bind the affinity label and that the reduced signal was due to quenching in the ^{14}C-FSBA labeling experiments.

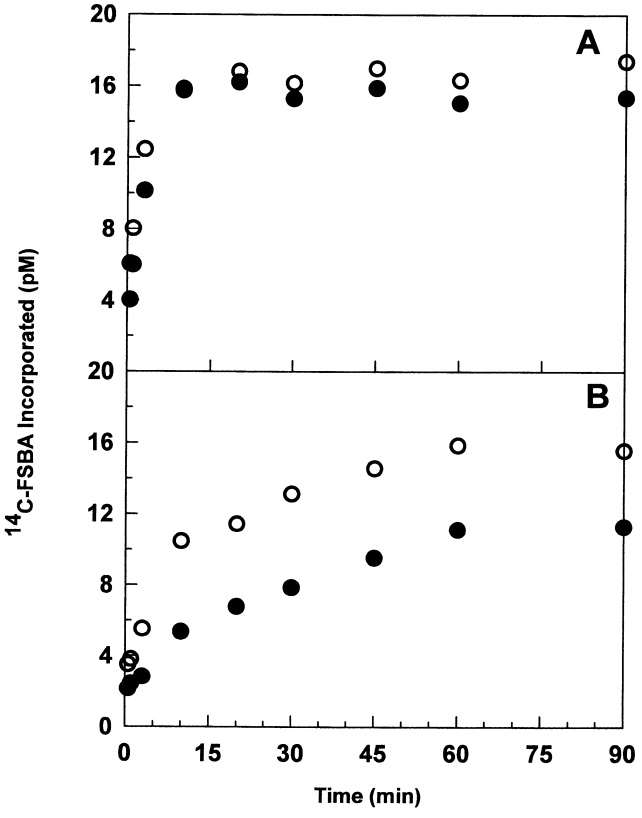

Fig. 2. 14C-FSBA Incorporation into p38γ MAP kinase. A: Unphosphorylated enzyme in the absence (○) and presence (●) of 1.2 mM AMP-PCP. B: Activated enzyme in the absence (○) and presence (●) of 1.2 mM AMP-PCP

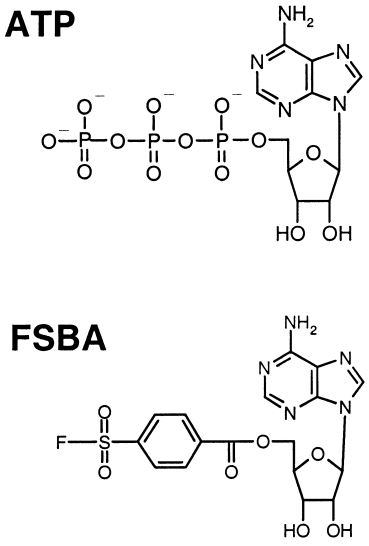

Fig. 3. Structures of ATP and FSBA.

4. Discussion

Structural information for p38α, ERK2, JNK3, and most recently p38γ [25], MAP kinases has provided an excellent understanding of MAP kinase activation and inhibition. In contrast, details of the catalytic mechanism has been lacking, with only one report directly addressing the kinetic mechanism for a MAP kinase [23]. We have investigated the kinetic mechanism and ATP-binding site reactivity of p38γ, a closely related homolog of p38α. There is considerable conflicting data in the literature concerning the substrate specificity of p38γ and the effect of pyridinyl imidazole inhibitors on this enzyme [17,18,26]. Our observations that ATF2 was an effective substrate for p38_(Fig. 1C and Table 1) and that neither SB202190 or SB203580 exhibit any inhibition of p38γ, at concentrations up to 20 μM, clarifies some of the confusion. In addition, we identified three phosphorylation sites, Tyr-183 and Thr-185 in the activation lip, and Ser-3 near the N-terminal portion of the enzyme. Cuenda et al. [27] first reported that p38γ was phosphorylated at a third site, which they speculated could be Ser-3 and/or Ser-281, which both precede

a Pro residue. Our data demonstrate that Ser-3, but not Ser-281, is phosphorylated and that this is an autophosphorylation event catalyzed by activated p38γ. Furthermore, phosphorylation of Ser-3 had no effect on the enzymatic activity of activated p38γ,.

The identification of significant ATPase activity for p38γ led us to probe other MAP kinases for a similar ability to turn over ATP in the absence of a phosphoacceptor substrate. ATPase activity was observed for all four MAP kinases tested (p38α, ERK2 and JNK3, in addition to p38γ). This observation suggests that formation of a binary E•MgATP complex is possible in the absence of a phosphoacceptor substrate. A published mechanism for p38α described ordered substrate binding with the phosphoacceptor substrate binding first [23], but in light of our data in Fig. 1 and Table 2, such a mechanism can be ruled out for p38α, p38γ, ERK2 and JNK3. These data indicate that the phosphoacceptor can not bind first. Substrate binding to p38γ involves either ATP binding first, or random substrate binding, although these data do not allow us to distinguish between the two latter mechanisms.

Because of the apparent contradiction between our data and those determined for p38α [23], we sought additional experiments to study the ability of ATP to bind p38γ in the absence of a phosphoacceptor. FSBA modification and competition experiments with AMP-PCP provide further insight into the ATP-binding site reactivity of this enzyme. FSBA is an effective affinity label for the EGF receptor kinase [24,28,29] and we found that it efficiently and selectively modified the ATP site of p38γ MAP kinase. FSBA and AMP-PCP differ structurally only in the triphosphate region (Fig. 3), so it is interesting that FSBA binds more rapidly to unphosphorylated p38γ, i.e. the form which appears unable to bind AMP-PCP. FSBA reactivity was also found to be independent of Mg^{2+} while AMP-PCP, as one might expect, required Mg^{2+} to bind and protect activated p38γ against FSBA inactivation.

FSBA reactivity can be understood in the context of the existing MAP kinase structures. The structures of activated ERK2 and p38γ and of unphosphorylated p38α, ERK2 and JNK3 have been determined [25,30–33]. While a comparison of activated and unphosphorylated p38γ would be most relevant to this study, the structure of unphosphorylated p38γ has not been determined. p38α shares a high degree of sequence identity with p38γ and so the structure of unphosphorylated p38α can be compared with activated p38γ. The structures of activated ERK2 and p38γ are almost identical to one another and are characterized most generally by a closure of the two kinase domains (relative to the unphosphorylated state). ATP binds p38γ at the interface between these two domains and this closure helps align the catalytic residues that coordinate the ATP and Mg^{2+} ions. All of the existing unphosphorylated MAP kinase structures show the two kinase domains opened to differing extents relative to the activated state. Unphosphorylated p38α is the most open relative to activated p38γ and ERK2, and differs by about 20° from the activated state. It seems reasonable that such a large conformational difference between the unphosphorylated and activated states of p38γ could modulate the ability of FSBA and other ATP analogs bind the active site. FSBA more readily binds to the open unphosphorylated state of p38γ compared to the closed activated form. The open unphosphorylated state does not appear to bind AMP-PCP and thus AMP-PCP can not compete with FSBA binding. AMP-PCP can however compete with binding to the closed activated form, for which it has affinity. Additional competition experiments involving FSBA may be useful to further probe the different conformational states of these enzymes. There are clearly significant differences between MAP kinases. For example, ERK2 and JNK3 have both been shown to bind ATP or ATP analogs in the inactive state [30,33]. In contrast, unphosphorylated p38 members do not appear to bind ATP or the non-hydrolyzable analog, AMP-PCP.

We present data demonstrating that a phosphoacceptor substrate does not have to bind prior to ATP in activated p38α, p38γ, ERK2 and JNK3, since all of these enzymes exhibit significant basal ATPase activity. The unphosphorylated form of p38γ was unable to bind AMP-PCP unlike inactive ERK2 and JNK3, which were both capable of binding ATP or AMP-PCP. This suggests there may be significant structural differences between activation of members of the p38 class compared to the ERK and JNK classes. None of the MAP kinases in this study exhibited any measurable basal ATPase activity in the unphosphorylated state. This study improves our understanding of MAP kinase ATP-binding site reactivity and provides new insight into the kinetic mechanism of this family.

Acknowledgements: We thank Dr. Steve Bellon for insightful discussions and comments regarding MAP kinase structural data. We are grateful to Dr.'s Sam Pazhanisamy, Steve Bellon, Keith Wilson, John Thomson and Vicki Sato for their critical reading of this manuscript.

References

[1] Cobb, M.H. and Goldsmith, E.J. (1995) J. Biol. Chem. 270, 14843–14846.
[2] Davis, R.J. (1995) Mol. Reprod. Dev. 42, 459–467.
[3] Minden, A. and Karin, M. (1997) Biochim. Biophys. Acta 1333, 85–104.
[4] Bokemeyer, D., Sorokin, A. and Dunn, M.J. (1996) Kidney Int. 49, 1187–1198.
[5] Derijard, B., Hibi, M., Wu, I.H., Barrett, T., Su, B., Deng, T., Karin, M. and Davis, R.J. (1994) Cell 76, 1025–1037.
[6] Han, J., Lee, J.D., Bibbs, L. and Ulevitch, R.J. (1994) Science 265, 808–811.
[7] Shapiro, L. and Dinarello, C.A. (1995) Proc. Natl. Acad. Sci. USA 92, 12230–12234.
[8] Rouse, J., Cohen, P., Trigon, S., Morange, M., Alonso, L.A., Zamanillo, D., Hunt, T. and Nebreda, A.R. (1994) Cell 78, 1027–1037.
[9] Raingeaud, J., Whitmarsh, A.J., Barrett, T., Derijard, B. and Davis, R.J. (1996) Mol. Cell. Biol. 16, 1247–1255.
[10] van Dam, H., Wilhelm, D., Herr, I., Stetfen, A., Herrlich, P. and Anglel, P. (1995) EMBO J. 14, 1798–1811.
[11] Whitmarsh, A.J., Shore, P., Sharrocks, A.D. and Davis, R.J. (1995) Science 269, 403–407.
[12] Chen, R.H., Abate, C. and Blenis, J. (1993) Proc. Natl. Acad. Sci. USA 90, 10952–10956.
[13] Oliver, B.L., Sha'afi, R.I. and Hajjar, J.J. (1995) Proc. Soc. Exp. Biol. Med. 210, 162–170.
[14] Hibi, M., Lin, A., Smeal, T., Minden, A. and Karin, M. (1993) Genes Dev. 7, 2135–2148.
[15] Chow, C.W., Rincon, M., Cavanagh, J., Dickens, M. and Davies, R.J. (1997) Science 278, 1638–1641.
[16] Zhang, Y., Zhou, L. and Miller, C.A. (1998) Proc. Natl. Acad. Sci. USA 95, 2586–2591.
[17] Li, Z., Jiang, Y., Ulevitch, R.J. and Han, J. (1996) Biochem. Biophys. Res. Commun. 228, 334–340.
[18] Kumar, S., McDonnell, P.C., Gum, R.J., Hand, A.T., Lee, J.C. and Young, P.R. (1997) Biochem. Biophys. Res. Commun. 235, 533–538.

[19] Wilson, K.P., McCaffrey, P.G., Hsiao, K., Pazhanisamy, S., Galullo, V., Bemis, G.W., Fitzgibbon, M.J., Caron, P.R., Murcko, M.A. and Su, M.S-S. (1997) Chem. Biol. 4, 223–231.
[20] Fox, T., Coll, J.T., Xie, X., Ford, P.J., Germann, U.A., Porter, M.D., Pazhanisamy, S., Fleming, M.A., Galullo, V., Su, M.S-S. and Wilson, K.P. (1998) Protein Sci. 7, 1–7.
[21] Gonzalez, F.A., Raden, D.L. and Davis, R.J. (1991) J. Biol. Chem. 266, 22159–22163.
[22] Han, J., Lee, J.D., Jiang, Y., Li, Z., Feng, L. and Ulevitch, R.J. (1996) J. Biol. Chem. 271, 2886–2891.
[23] LoGrasso, P.V., Frantz, B., Rolando, A.M., O'Keefe, S.J., Hermes, J.D. and O'Neill, E.A. (1997) Biochemistry 36, 10422–10427.
[24] Scoggins, R.M., Summerfield, A.E., Stein, R.A., Guyer, C.A. and Staros, J.V. (1996) Biochemistry 35, 9197–9203.
[25] Bellon, S., Fitzgibbon, M.J., Fox, T., Hsiao, H.-M. and Wilson, K.P. (1999) Structure 7, 1057–1065.
[26] Cuenda, A., Cohen, P., Buee, S.V. and Goedert, M. (1997) EMBO J. 16, 295–305.
[27] Cuenda, A., Alonso, G., Morrice, N., Jones, M., Meier, R., Cohen, P. and Nebreda, A.R. (1996) EMBO J. 15, 4156–4164.
[28] Buhlow, S.A., Cohen, S. and Staros, J.V. (1982) J. Biol. Chem. 257, 4019–4022.
[29] Buhlow, S.A., Cohen, S., Garbers, D.L. and Staros, J.V. (1983) J. Biol. Chem. 258, 7824–7827.
[30] Zhang, F., Strand, A., Robbins, D., Cobb, M.H. and Goldsmith, E.J. (1994) Nature 367, 704–711.
[31] Wilson, K.P., Fitzgibbon, M.J., Caron, P.R., Griffith, J.P., Chen, W., McCaffrey, P.G., Chambers, S.P. and Su, M.S. (1996) J. Biol. Chem. 271, 27696–27700.
[32] Wang, Z., Harkins, P.C., Ulevitch, R.J., Han, J., Cobb, M.H. and Goldsmith, E.J. (1997) Proc. Natl. Acad. Sci. USA 94, 2327–2332.
[33] Xie, X., Gu, Y., Fox, T., Coll, J.T., Fleming, M.A., Markland, W., Caron, P.R., Wilson, K.P. and Su, M.S-S. (1998) Structure 6, 983–991.